

UV-Induced Proton Transfer between DNA Strands

Yuyuan Zhang,[†] Kimberly de La Harpe,[‡] Ashley A. Beckstead,[†] Roberto Improta,^{*,§} and Bern Kohler^{*,†}

[†]Department of Chemistry and Biochemistry, Montana State University, Bozeman, Montana 59717, United States

[‡]Department of Physics, United States Air Force Academy, USAF Academy, Colorado 80840, United States

[§]Consiglio Nazionale delle Ricerche, Istituto di Biostrutture e Bioimmagini, Via Mezzocannone 16, 80136 Naples, Italy

Supporting Information

ABSTRACT: UV radiation creates excited states in DNA that lead to mutagenic photoproducts. Photoexcitation of single-stranded DNA can transfer an electron between stacked bases, but the fate of excited states in the double helix has been intensely debated. Here, photoinduced interstrand proton transfer (PT) triggered by intrastrand electron transfer (ET) is detected for the first time by time-resolved vibrational spectroscopy and quantum mechanical calculations. Long-lived excited states are shown to be oppositely charged base pair radical ions. In two of the duplexes, the base pair radical anions are present as tautomers formed by interstrand PT. Charge recombination occurs on the picosecond time scale preventing the accumulation of damaging radicals or mutagenic tautomers.

Solar UV radiation triggers damaging reactions in DNA that can lead to mutations. Single nucleobases have subpicosecond excited state lifetimes that are thought to minimize the likelihood of photochemical reactions. Surprisingly, excited states of DNA strands can decay orders of magnitude more slowly.^{1–3} Recent studies have confirmed that radical ion pairs with lifetimes of tens to hundreds of picoseconds are formed in single-stranded DNA by photoinduced electron transfer (ET) between stacked nucleobases.^{4–6} Picosecond lifetimes have also been observed in double-stranded DNA,^{1,3,7} but a recent study suggests that charge transfer (CT) states seen in single DNA strands are suppressed by the Watson–Crick hydrogen bonds between bases in the double helix.³ Despite intense experimental and theoretical effort over the past decade, the mechanism behind slower energy relaxation in double-stranded DNA remains highly uncertain.

Intrastrand electron transfer can potentially trigger interstrand proton transfer as illustrated in Figure 1. Here we show by femtosecond time-resolved IR (TRIR) spectroscopy and quantum mechanical calculations that long-lived excited states in three representative DNA duplexes are CT states formed when an electron–hole pair is generated on one strand of a DNA duplex. In two of the three duplexes, an electron moves between adjacent bases on the same strand, attracting a proton from the opposite strand (Figure 1b), yielding a rare tautomeric base pair that decays in under 1 ns. This distinctive proton-coupled electron transfer (PCET) mechanism differs from the landmark theoretical proposal of Sobolewski and Domcke^{8,9} in which the electron and proton originate from the same base in a single base

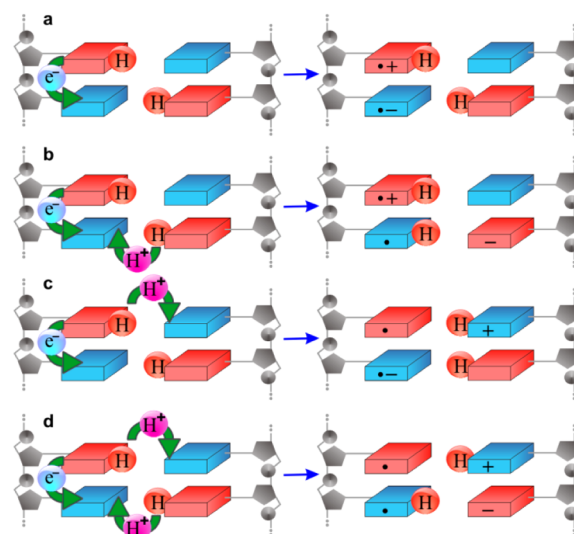


Figure 1. Proposed electron and proton movement in DNA stacked base pairs following UV excitation. Intrastrand ET (a–d) can occur without PT (a), or with PT in the base pair radical anion (b), base pair radical cation (c), or in both base pair radical ions (d).

pair. To our knowledge, this is the first observation of photoinduced proton transfer (PT) in DNA.

Radical ions of single nucleobases are considerably stronger acids and bases than their parent molecules.^{10,11} They undergo PT reactions with water molecules, but at rates that are too slow ($<10^8 \text{ s}^{-1}$)^{12,13} to influence the subnanosecond excited-state lifetimes observed in double-stranded DNA. PT can occur orders of magnitude faster in base pairs between a radical ion nucleobase and its neutral complement because the latter is usually a much stronger acid or base than a water molecule. Single PT can occur in one or both of the base pair radical ions generated by intrastrand ET, transforming an initial radical ion into a neutral radical and causing the complementary base to acquire a charge through deprotonation (Figure 1b) or protonation (Figure 1c). ET/PT thus separates spin from charge in a base pair, yielding distonic radical ions.¹⁴ The overall mechanism is an example of multiple site PCET.¹⁵

PT is predicted to be exergonic for three of the four base pair radical anions from experimental acid dissociation constants (see Supporting Information, SI). The favorable Coulomb attraction

Received: April 15, 2015

Published: May 25, 2015

from moving a proton on one strand toward the electron on the other strand (Figure 1b) suggests that PT could take place on an ultrafast time scale in most base pair radical anions, but is less likely in base pair radical cations, consistent with previous computational results.^{16–18} Double PT in radical ion base pairs is not expected on energetic grounds.¹⁷

Vibrational spectra were recorded for three duplexes with the base sequences shown in Figures 2 and 3 in buffered D₂O

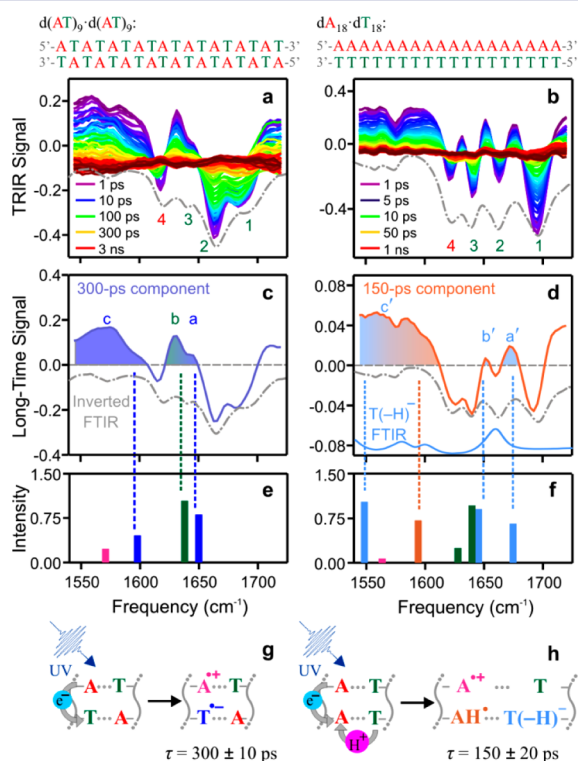


Figure 2. (a,b) TRIR spectra of $d(AT)_9 \cdot d(AT)_9$ and $dA_{18} \cdot dT_{18}$ at the indicated delay times following 265 nm excitation in D₂O solution at 7 °C. (c,d) The difference spectra of the longest-lived signal components determined by global fitting compared with the inverted FTIR spectra and, in panel d, the FTIR spectrum of the deprotonated T monomer. (e,f) PCM/M052X/6-31G(d) calculated frequencies (scaled by 0.95) for the radical ion pairs shown in panels g and h.

solution after excitation with 100 fs, 265 nm laser pulses (melting curves and steady-state spectroscopic results are shown in Figure S1). TRIR spectra are difference spectra consisting of negative bands due to the bleaching of ground-state vibrations and positive ones arising from vibrational modes of new states formed by excitation. The negative bands align well with valleys in the inverted steady-state FTIR spectrum of each duplex. The difference spectrum of the longest decay component was determined by global analysis and is shown for the A·T duplexes in Figure 2c,d and for the G·C duplex in Figure 3b (other decay components are in Figure S2).

Despite containing identical numbers of A·T base pairs, the TRIR spectra of $d(AT)_9 \cdot d(AT)_9$ and $dA_{18} \cdot dT_{18}$ are strikingly different in appearance (Figure 2a,b). In $d(AT)_9 \cdot d(AT)_9$, a strong positive band is seen at 1630 cm⁻¹ between ground-state bands 3 and 4 that has no counterpart in the $dA_{18} \cdot dT_{18}$ duplex. However, positive maxima appear in the difference spectrum of $dA_{18} \cdot dT_{18}$ at 1653 and 1672 cm⁻¹, which are much less prominent in the alternating duplex. The long-time difference spectrum of $d(AT)_9 \cdot d(AT)_9$ (Figure 2c) decays with a lifetime of

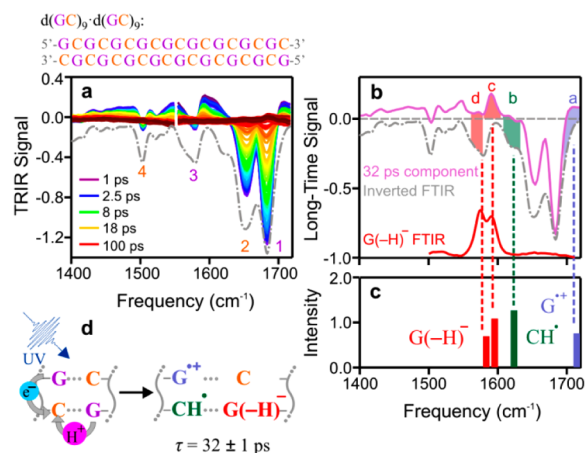


Figure 3. (a) TRIR spectra of $d(GC)_9 \cdot d(GC)_9$ at the indicated delay times following 265 nm excitation in D₂O solution. (b) The difference spectrum of the longest signal component determined by global fitting compared with the inverted FTIR spectrum and the FTIR spectrum of the deprotonated G monomer. (c) PCM/M052X/6-31G(d) calculated frequencies (scaled by 0.95) for vibrations of the PCET state illustrated in panel d.

300 ± 10 ps, while that of $dA_{18} \cdot dT_{18}$ (Figure 2d) has a lifetime of 150 ± 20 ps. This contrasts with the report by Bucher et al.³ of a single 210 ps lifetime for ground-state vibrational marker bands of A·T base pairs in calf thymus DNA. The different lifetimes and spectral signatures reveal that excited states of these isomeric duplexes arise from interactions in at least two stacked base pairs.

To assign the positive features, the observed frequencies were compared with harmonic frequencies calculated for two stacked base pairs including the phosphate-deoxyribose backbone and sodium counterions (see SI). Calculating excited-state vibrational frequencies is prohibitively expensive so a cost-effective procedure, already applied successfully to single-stranded DNAs,^{4–6,19} was adopted. In this procedure, the vibrational spectrum of each CT excited state was approximated by the sum of vibrational spectra of the separate base pair radical ions in their *ground* electronic states. Each base pair radical ion (whether distonic or not) was part of a base tetramer that included a neutral base pair in order to capture secondary effects on the vibrational spectra due to base stacking (Figure S3). Calculations were carried out using density functional theory and the M052X functional, which gives a reliable description of stacking interactions.²⁰

For the B-form $d(AT)_9 \cdot d(AT)_9$ duplex, vibrational marker bands diagnostic of an A^{•+}·T base pair stacked with a T^{•-}·A base pair are evident in the long-time difference spectrum. The vibrational frequencies calculated for the model $d(AT) \cdot d(AT)$ base pair dimer, assuming that PT does not take place in either of the resulting base pair radical ions, are shown by the sticks in Figure 2e. The sticks are colored to match the bases in panel g, showing the primary site of each vibrational normal mode. Due to coupling of vibrational modes of different bases^{21,22} the assignments are necessarily qualitative. The absence of photo-induced PCET in the alternating A·T duplex is consistent with thermodynamic estimates (see SI). PT is endergonic in the A·T^{•-} base pair because of the low acidity of A and the low basicity of T^{•-}.

In contrast, the longest-lived excited state of the non-alternating B-form $dA_{18} \cdot dT_{18}$ duplex shows the signature vibrational bands of an A^{•+}·T base pair radical cation and the

$A(+H1)^{\bullet} \cdot T(-H3)^{-}$ distonic radical anion. The IR spectrum of the closed-shell anion $T(-H3)^{-}$ was recorded in D_2O solution and compared with calculations. At high pH, the N3 proton of the T monomer is lost (the same proton that transfers from T to $A^{\bullet-}$) and a single band appears in D_2O solution at 1660 cm^{-1} in place of the trio of bands for neutral T between 1630 and 1700 cm^{-1} (FTIR spectrum in Figure 2d). This band, which is nearly unaffected by duplex formation, is predicted to occur at 1675 cm^{-1} in agreement with band a' in Figure 2d. The C2O carbonyl stretch of $T(-H3)^{-}$, which occurs below 1630 cm^{-1} in the monomer, is predicted at 1648 cm^{-1} in the duplex, in agreement with band b' in Figure 2d. The calculated C4O stretch of $T(-H3)^{-}$ at 1549 cm^{-1} and a mode of $A(+H1)^{\bullet}$ at 1595 cm^{-1} are in good agreement with the broad positive band c' in Figure 2d. The distinctive marker bands of $T(-H3)^{-}$ and $A(+H1)^{\bullet}$ provide clear evidence of a distonic base pair radical anion generated by interstrand PT and $A \rightarrow A$ intrastrand ET.

Photoinduced PCET is also observed in the alternating B-form $d(GC)_9 \cdot d(GC)_9$ duplex made of 18 G·C base pairs. The TRIR signals (Figure 3a) decay biexponentially with lifetimes of 7.6 ± 0.4 and 32 ± 1 ps, similar to ones reported for poly(dGdC)·poly(dGdC).²³ The slow component, which is again our focus, has the difference spectrum shown in Figure 3b. Photoexcitation is proposed to transfer an electron from G to a neighboring C on the same strand, simultaneously forming stacked $G^{\bullet+} \cdot C$ and $C^{\bullet-} \cdot G$ base pairs. Experimental acid dissociation constants predict that the distonic form of the latter base pair $C(+H3)^{\bullet} \cdot G(-H1)^{-}$ lies lower in energy (see SI). Interstrand $G \rightarrow C$ CT does not appear to take place as such states lie $\sim 0.8\text{ eV}$ above intrastrand $G \rightarrow C$ ET states at the Franck–Condon geometry.²⁴

The FTIR spectrum of the monomer $G(-H1)^{-}$ (red curve in Figure 3b) has two strong bands around 1595 cm^{-1} near bands c and d in the experimental difference spectrum. Both bands occur at similar frequencies for $G(-H1)^{-}$ in a duplex, according to our calculations. The calculated carbonyl stretching frequency of the $C(+H3)^{\bullet}$ neutral radical matches band b in Figure 3b, confirming that the N1 proton of G is transferred along the middle hydrogen bond to the N3 atom of $C^{\bullet-}$. The band observed at $\sim 1700\text{ cm}^{-1}$ (band a) was assigned previously to the carbonyl stretch of $G^{\bullet+}$ from TRIR experiments on single-stranded DNA oligomers⁵ and monomers at room temperature²⁵ and at 77 K .²⁶ Single PT does not appear to take place in the $G^{\bullet+} \cdot C$ base pair likely because of the reduced exergonicity.

We have thus identified three vibrational bands for three transient species $G^{\bullet+}$, $C(+H3)^{\bullet}$, and $G(-H1)^{-}$, which can only be generated when a single C residue acts as an electron–proton acceptor following UV excitation. Notably, a larger fraction of all excited states in the alternating G·C duplex decay by PCET than is the case in the nonalternating A·T duplex based on the smaller amplitude of the long-lived signal in the latter system (Figure S2). Interstrand CT states are predicted by calculations to be more accessible in duplexes with nonalternating vs alternating base sequence,^{24,27} and such states may decay on an ultrafast time scale.^{8,9} Ultrafast relaxation to the ground state is known to occur competitively with the formation of long-lived excited states in DNA.²⁸

Our assignments for the long-lived excited states observed in the A·T and G·C duplexes are summarized in Figure 4. Other ET/PT possibilities, including interstrand H atom transfer, were considered for the three duplexes (Figures S4–S6), but the vibrational frequencies calculated for alternative states fail to match the patterns of experimentally observed bands. Importantly, the vibrational marker bands used to identify the

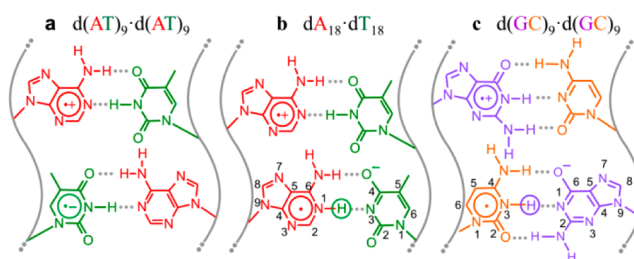


Figure 4. Long-lived excited states observed in three DNA duplexes. (a) Intrastrand CT state in the alternating A·T duplex. (b,c) Base pair radical ions in the nonalternating A·T and alternating G·C duplexes, respectively. Tautomerization has taken place in the lower base pair by transfer of the circled proton from the base on the right to the base on the left.

long-lived excited states in both the A·T and G·C duplexes show no growth kinetics. The ET and PT steps that yield distonic radical ions must therefore occur very close together in time. Unfortunately, the strong signals seen at short times make it difficult to determine whether PCET takes place via a concerted mechanism or via rapid sequential transfers.

After the photoinduced PCET reaction, both electron and proton return to their starting locations, preventing photo-damage. Back ET/back PT may occur concertedly given that the long-time difference spectrum, which we have assigned to a base pair tautomer, decays with a single lifetime. However, rate-limiting back ET between the two radicals on the same strand followed by ultrafast PT between the resulting closed-shell and oppositely charged ions could also account for the observed kinetics. By lowering the energy gap between the excited state and the ground state, PT in radical ion base pairs could accelerate the decay of the CT state. This is our proposed explanation for the approximately 2-fold decrease in lifetime for the CT state of a nonalternating AT duplex compared to the CT state of single-stranded $(dA)_{18}$.²⁸

In summary, tautomeric base pairs have been detected by matching experimental marker bands with frequencies calculated for base pair radical ions in their ground electronic states. The excellent agreement between experiment and theory validates the assumption that the underlying ET or ET/PT states are energetically accessible. Excited-state calculations exploring the energetics of the CT states are a desirable next step that can shed light on whether ET and PT reactions take place concertedly or sequentially.

The photoinduced PCET mechanism identified here reveals the importance of both base pairing and base stacking interactions. Because ET rates decay exponentially with distance, maximal rates are observed when electron donor and acceptor groups are in van der Waals contact,²⁹ the precise geometry encountered in stacked nucleobases. Base pairing further provides the pre-existing hydrogen bonds required for ultrafast PT. The DNA double helix can thus be viewed as a continuous sequence of electron and proton donor–acceptor junctions that favor short-range ET/PT reactions between nucleobases in stacked base pairs upon photoexcitation. The strong Coulomb attraction experienced by bound and possibly highly localized electron–hole pairs in stacked DNA base pairs frustrates their dissociation, preventing the accumulation of long-lived base pair tautomers that could cause mutations.³⁰

This study reveals intriguing connections between UV excited states of DNA and charge carrier generation and transport in DNA.³¹ The base pair radical ions observed in this study behave

similarly to ones formed when DNA interacts with ionizing radiation.^{11,32} The ability to observe and study photoinduced PCET in DNA offers exciting opportunities to elucidate the fundamental principles that govern energy and charge migration in multichromophoric systems made of organic building blocks, systems that play a central role in biological and biomimetic energy harvesting and photocatalysis.³³

■ ASSOCIATED CONTENT

📄 Supporting Information

Experimental and computational methods, supplemental text. The Supporting Information is available free of charge on the ACS Publications website at DOI: 10.1021/jacs.5b03914.

■ AUTHOR INFORMATION

Corresponding Authors

*robimp@unina.it

*kohler@chemistry.montana.edu

Notes

The authors declare no competing financial interest.

■ ACKNOWLEDGMENTS

Work at Montana State University was supported by NSF (CHE-1112560) and NASA (NNX12AG77G). The TRIR spectrometer was constructed with funding from the M. J. Murdock Charitable Trust. R.I. was supported by the Italian Ministero dell'Istruzione, dell'Università e della Ricerca (MIUR Grants PRIN-2010ERFKXL), and French Agency for Research Grant ANR-12-BS08-0001-01. The TOC graphic was prepared using the UCSF Chimera package.³⁴

■ REFERENCES

- (1) Crespo-Hernández, C. E.; Cohen, B.; Kohler, B. *Nature* **2005**, *436*, 1141.
- (2) Markovitsi, D.; Gustavsson, T.; Vayá, I. *J. Phys. Chem. Lett.* **2010**, *1*, 3271.
- (3) Bucher, D. B.; Schlueter, A.; Carell, T.; Zinth, W. *Angew. Chem., Int. Ed.* **2014**, *53*, 11366.
- (4) Doorley, G. W.; Wojdyla, M.; Watson, G. W.; Towrie, M.; Parker, A. W.; Kelly, J. M.; Quinn, S. J. *J. Phys. Chem. Lett.* **2013**, *4*, 2739.
- (5) Bucher, D. B.; Pilles, B. M.; Carell, T.; Zinth, W. *Proc. Natl. Acad. Sci. U.S.A.* **2014**, *111*, 4369.
- (6) Zhang, Y.; Dood, J.; Beckstead, A. A.; Li, X. B.; Nguyen, K. V.; Burrows, C. J.; Improta, R.; Kohler, B. *Proc. Natl. Acad. Sci. U.S.A.* **2014**, *111*, 11612.
- (7) de La Harpe, K.; Kohler, B. *J. Phys. Chem. Lett.* **2011**, *2*, 133.
- (8) Sobolewski, A. L.; Domcke, W. *Phys. Chem. Chem. Phys.* **2004**, *6*, 2763.
- (9) Perun, S.; Sobolewski, A. L.; Domcke, W. *J. Phys. Chem. A* **2006**, *110*, 9031.
- (10) Steenzen, S. *Free Radical Res. Commun.* **1992**, *16*, 349.
- (11) Kumar, A.; Sevilla, M. D. *Chem. Rev.* **2010**, *110*, 7002.
- (12) Kobayashi, K.; Tagawa, S. *J. Am. Chem. Soc.* **2003**, *125*, 10213.
- (13) Yamagami, R.; Kobayashi, K.; Tagawa, S. *J. Am. Chem. Soc.* **2008**, *130*, 14772.
- (14) Yates, B. F.; Bouma, W. J.; Radom, L. *J. Am. Chem. Soc.* **1984**, *106*, 5805.
- (15) Huynh, M. H. V.; Meyer, T. J. *Chem. Rev.* **2007**, *107*, 5004.
- (16) Colson, A.-O.; Besler, B.; Close, D. M.; Sevilla, M. D. *J. Phys. Chem.* **1992**, *96*, 661.
- (17) Bertran, J.; Oliva, A.; Rodríguez-Santiago, L.; Sodupe, M. *J. Am. Chem. Soc.* **1998**, *120*, 8159.
- (18) Li, X.; Cai, Z.; Sevilla, M. D. *J. Phys. Chem. B* **2001**, *105*, 10115.

- (19) Zhang, Y.; Dood, J.; Beckstead, A. A.; Li, X. B.; Nguyen, K. V.; Burrows, C. J.; Improta, R.; Kohler, B. *J. Phys. Chem. B* **2015**, DOI: 10.1021/jp511220x.
- (20) Zhao, Y.; Truhlar, D. G. *Acc. Chem. Res.* **2008**, *41*, 157.
- (21) Krummel, A. T.; Mukherjee, P.; Zanni, M. T. *J. Phys. Chem. B* **2003**, *107*, 9165.
- (22) Peng, C. S.; Jones, K. C.; Tokmakoff, A. *J. Am. Chem. Soc.* **2011**, *133*, 15650.
- (23) Doorley, G. W.; McGovern, D. A.; George, M. W.; Towrie, M.; Parker, A. W.; Kelly, J. M.; Quinn, S. J. *Angew. Chem., Int. Ed.* **2009**, *48*, 123.
- (24) Ko, C.; Hammes-Schiffer, S. *J. Phys. Chem. Lett.* **2013**, *4*, 2540.
- (25) Kuimova, M. K.; Cowan, A. J.; Matousek, P.; Parker, A. W.; Sun, X. Z.; Towrie, M.; George, M. W. *Proc. Natl. Acad. Sci. U.S.A.* **2006**, *103*, 2150.
- (26) Parker, A. W.; Lin, C. Y.; George, M. W.; Towrie, M.; Kuimova, M. K. *J. Phys. Chem. B* **2010**, *114*, 3660.
- (27) Lange, A. W.; Herbert, J. M. *J. Am. Chem. Soc.* **2009**, *131*, 3913.
- (28) Chen, J.; Thazhathveetil, A. K.; Lewis, F. D.; Kohler, B. *J. Am. Chem. Soc.* **2013**, *135*, 10290.
- (29) Moser, C. C.; Keske, J. M.; Warncke, K.; Farid, R. S.; Dutton, P. L. *Nature* **1992**, *355*, 796.
- (30) Löwdin, P. O. *Rev. Mod. Phys.* **1963**, *35*, 724.
- (31) Lewis, F. D.; Wasielewski, M. R. *Pure Appl. Chem.* **2013**, *85*, 1379.
- (32) Black, P. J.; Bernhard, W. A. *J. Phys. Chem. B* **2012**, *116*, 13211.
- (33) Gust, D.; Moore, T. A.; Moore, A. L. *Acc. Chem. Res.* **2001**, *34*, 40.
- (34) Pettersen, E. F.; Goddard, T. D.; Huang, C. C.; Couch, G. S.; Greenblatt, D. M.; Meng, E. C.; Ferrin, T. E. *J. Comput. Chem.* **2004**, *25*, 1605.